Electronic Supplementary Material (ESI) for Physical Chemistry Chemical Physics.

SUPPLEMENTARY INFORMATION

Percolation behaviors of ionic and electronic transfers in $Li_{3-2x}Co_xN$

J.C. Badot *[1,4], E. Panabière [2], N. Emery [2], O. Dubrunfaut [3],
S. Bach [2], and J.P. Pereira-Ramos [2]

[1] Chimie ParisTech, PSL Research University, CNRS,
Institut de Recherche de Chimie Paris, 75005 Paris, France
[2] Institut de Chimie et des Matériaux Paris-Est, CNRS, Groupe d'Electrochimie et Spectroscopie des Matériaux (GESMAT), 2-8, rue Henri Dunant - 94320 Thiais, France
[3] GeePs |Group of Electrical Engineering - Paris, UMR CNRS 8507, CentraleSupélec, Sorbonne Universités, UPMC Univ Paris 06, Univ Paris-Sud, Université Paris-Saclay, 11 rue Joliot-Curie, 91192 Gif-sur-Yvette, France
[4] Réseau sur le Stockage Electrochimique de l'Energie (RS2E), FR CNRS 3459, France
[5] Université d'Evry Val d'Essonne, Dept Chimie, Bd F. Mitterrand, 91000 Evry

S1. Dielectric spectroscopy device used for measurements from 60 Hz to 10 GHz

Complex permittivity and conductivity of $Li_{3-2x}Co_xN$ were measured by the broadband dielectric spectroscopy (BDS) from 60 to 10^{10} Hz, using simultaneously a network analyzer Agilent PNA E8364B (10^7 to 10^{10} Hz), two impedance analyzers Agilent 4294 (60 to 1.1×10^8 Hz) and Agilent 4291 (10^6 to 1.8×10^9 Hz). The experimental device consists of a coaxial cell (APC7 standard), in which the cylindrically shaped sample (diameter = 3 mm and thickness ≈ 1 mm) fills the gap between the inner conductor and a short-circuit (Fig. S1).

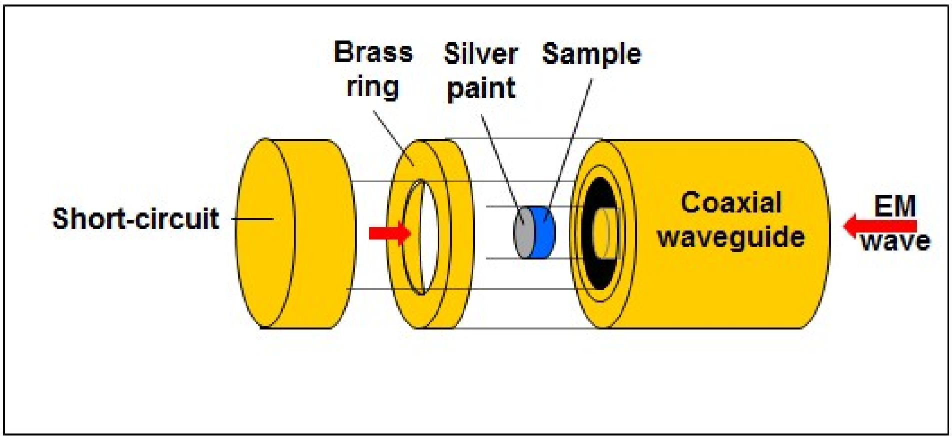

Figure S1 . Schema of the cell for dielectric measurements between 60 and 10^{10} Hz

The sample is covered with a silver paint on its two opposite sides to have good electrical contacts with coaxial waveguide. The brass ring allows to ensure the electrical continuity of the outer-conductor of the coaxial waveguide.

S2. Determination of ionic and electronic conductivities of $Li_{3-2x}Co_xN$ grains

Conductivity Nyquist plots of $Li_{3-2x}Co_xN$ (x = 0, 0.05 and 0.18)

Conductivity Nyquist plots (σ” vs. σ’) are more obvious than the resistivity Nyquist plots (ρ” vs. ρ’) in some cases (see Fig. S2). The grain bulk conductivity is plotted by a straight line in the conductivity complex plane. This straight line can be transformed by inversion into a circular arc which passes through the origin in the resistivity complex plane. Hence, it sometimes easier to draw a straight line than a circular arc in higher frequency range.

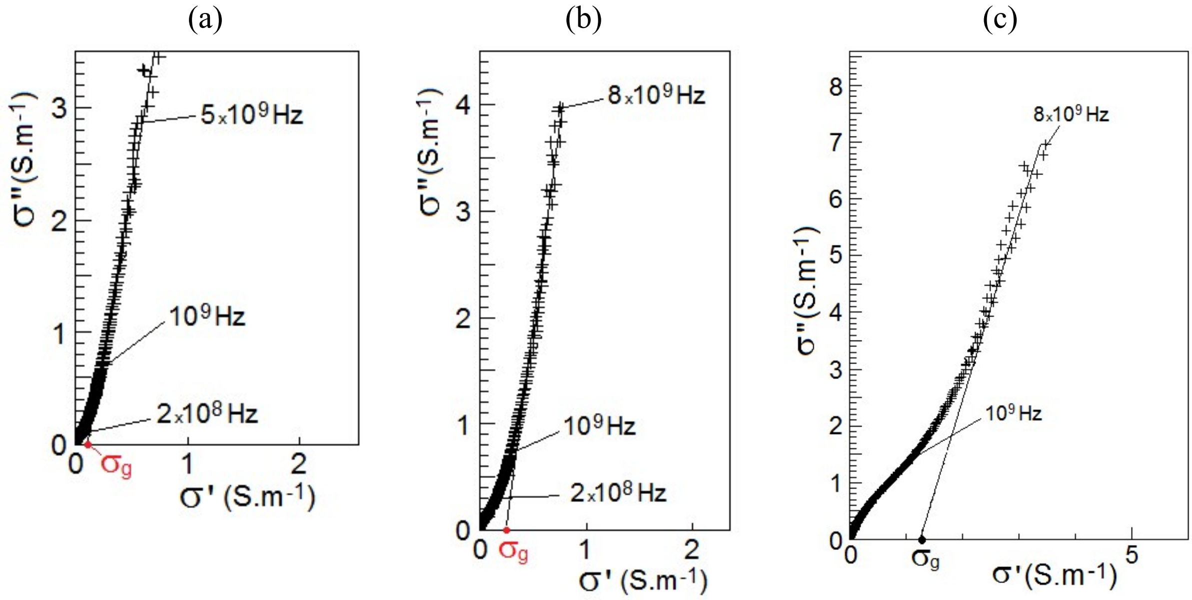

Figure S2. High frequency part of complex conductivity Nyquist plots (σ”(ω) vs. σ’(ω)) for the samples: a) Li_3N (LCN0), b) $Li_{2.9}Co_{0.05}N$ (LCN1) and c) $Li_{2.64}Co_{0.18}N$ (LCN4) at 300 K: evidence of straight line giving the grain conductivity σ_g.

Resistivity Nyquist plots of $Li_{3-2x}Co_xN$ (x = 0.25)

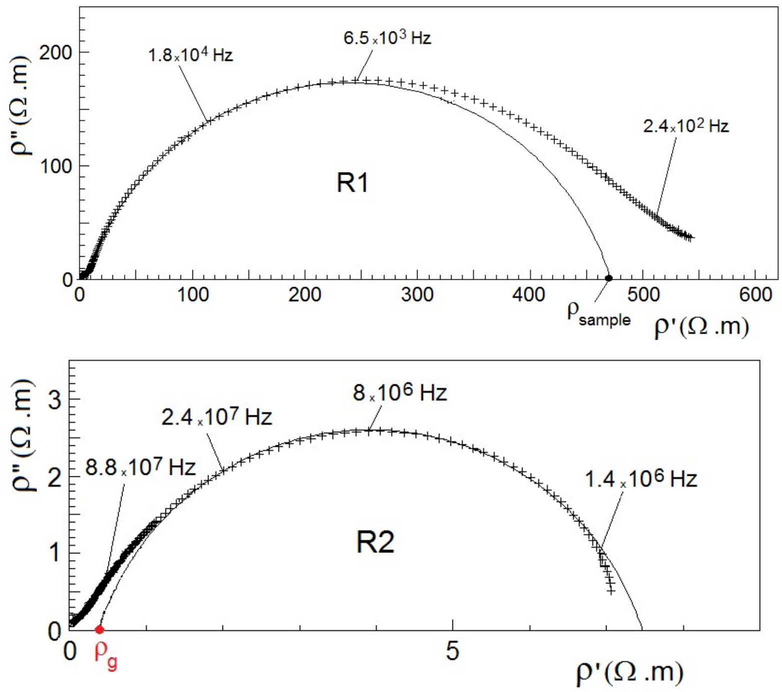

Figure S3. Complex resistivity Nyquist plots (ε"(ω) vs. ε'(ω))for the sample $Li_{2.5}Co_{0.25}N$ at 300 K: a) evidence of the relaxation domain R1 (particle/particle contacts) in the entire plot from 40 to 10^{10} Hz *(the deviation from R1 is due to contact sample/silver paint in the lower frequency range)*; b) evidence of the relaxation domain R2 (grain/grain contacts). ρ_g is the grain resistivity inverse of the grain conductivity σ_g.

S3. Dielectric relaxations in $Li_{3-2x}Co_xN$ samples

Permittivity Nyquist plots of Li_3N

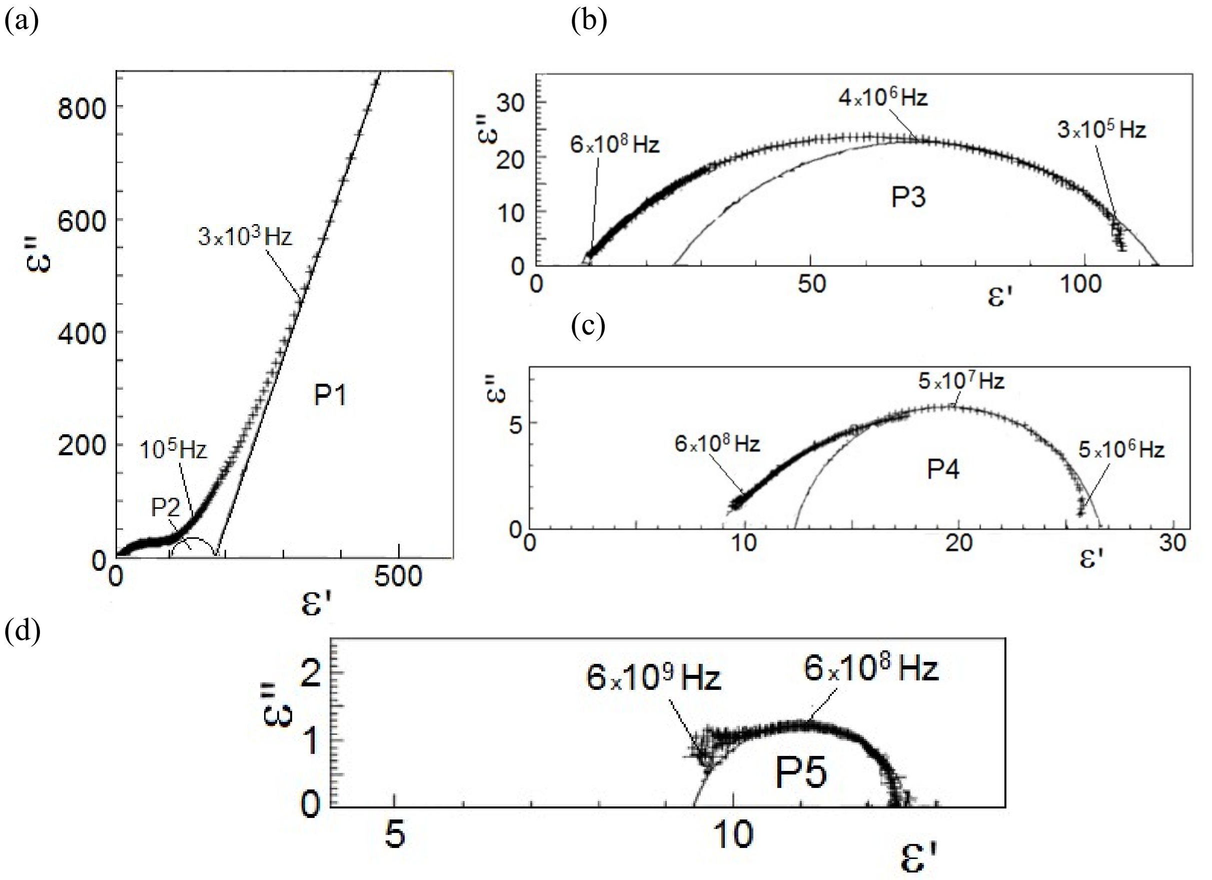

Figure S4. Nyquist plots of the imaginary part ε"(ω) vs. the real part ε'(ω) of the complex permittivity at 300 K for the sample Li_3N: a) entire plot from 40 to 10^{10} Hz: only the low frequency contribution P1 is visible; b) plot obtained upon subtracting the domain P1: evidence of the relaxation domains P2 (sample polarization) and P3 (particle polarization); c) plot obtained upon subtracting domains P2 and P3: evidence of the relaxation domain P4 (grain polarization); d) plot obtained upon subtracting the domain P4: evidence of the relaxation domain P5 (local Li^+ hopping).

Permittivity Nyquist plots of $Li_{2.50}Co_{0.25}N$

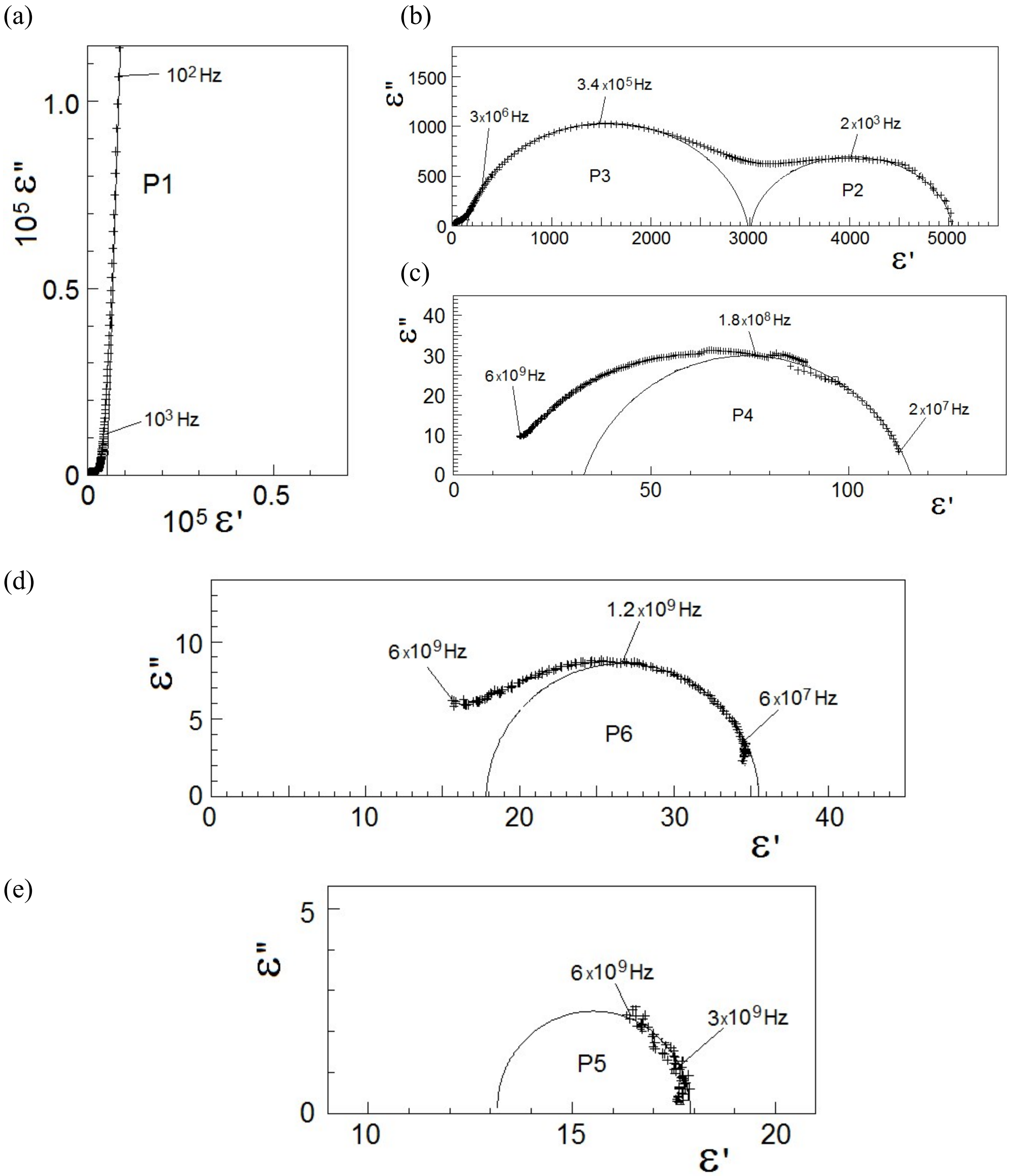

Figure S5. Nyquist plots of the imaginary part ε"(ω) vs. the real part ε'(ω) of the complex permittivity at 300 K for the sample $Li_{2.50}Co_{0.25}N$: a) entire plot from 40 to 10^{10} Hz: only the low frequency contribution P1 is visible; b) plot obtained upon subtracting the domain P1: evidence of the relaxation domains P2 (sample polarization) and P3 (particle polarization); c) plot obtained upon subtracting domains P2 and P3: evidence of the relaxation domain P4 (grain polarization); d) plot obtained upon subtracting the domain P4: evidence of the relaxation domain P5 (local Li^+ hopping); e) plot obtained upon subtracting the domain P5: evidence of the relaxation domain P6 (local electron hopping).

Permittivity Nyquist plots of $Li_{2.64}Co_{0.18}N$

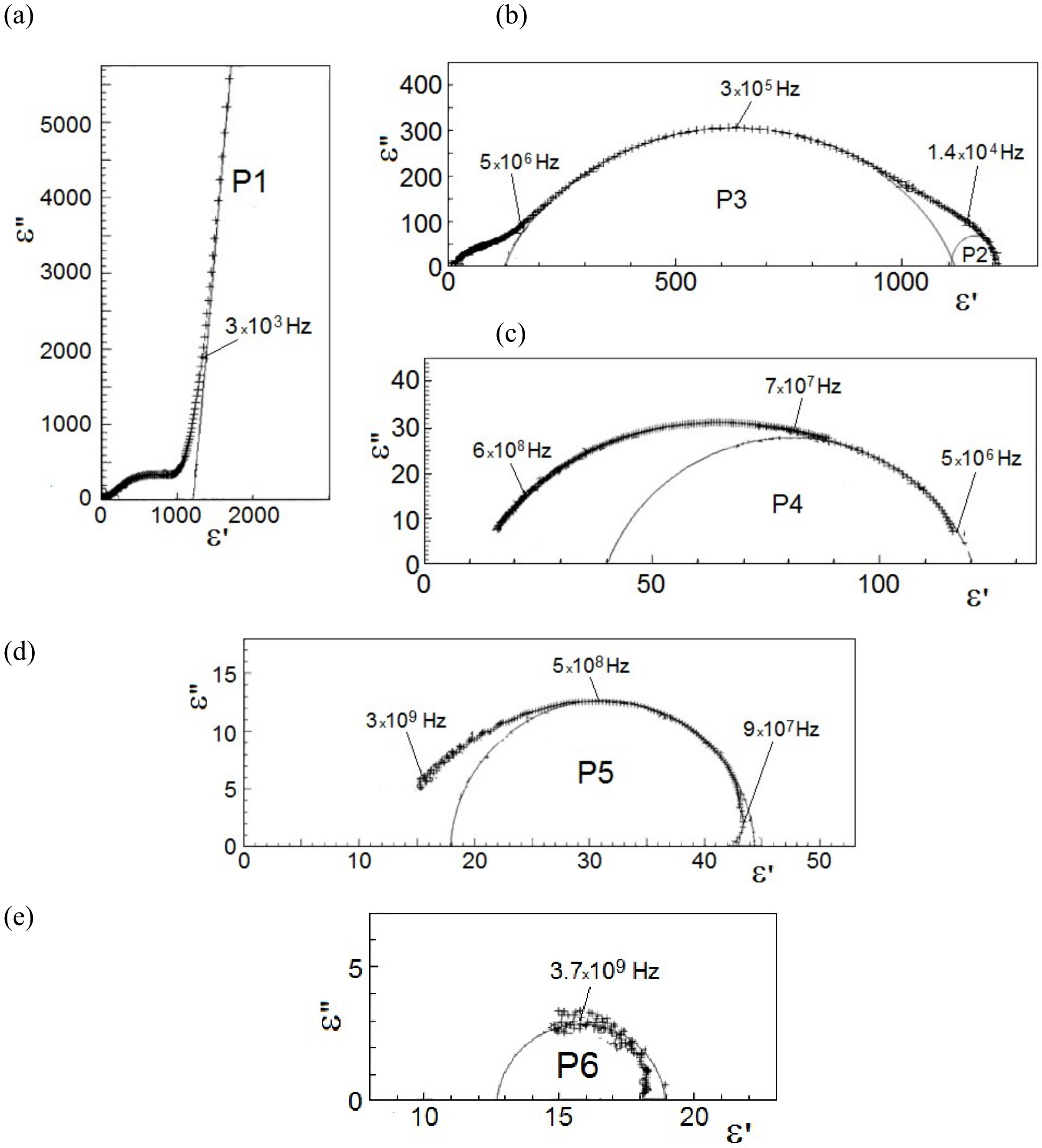

Figure S6. Nyquist plots of the imaginary part ε"(ω) vs. the real part ε'(ω) of the complex permittivity at 300 K for the sample $Li_{2.64}Co_{0.18}N$: a) entire plot from 40 to 10^{10} Hz: only the low frequency contribution P1 is visible; b) plot obtained upon subtracting the domain P1: evidence of the relaxation domains P2 (sample polarization) and P3 (particle polarization); c) plot obtained upon subtracting domains P2 and P3: evidence of the relaxation domain P4 (grain polarization); d) plot obtained upon subtracting the domain P4: evidence of the relaxation domain P5 (local Li^+ hopping); e) plot obtained upon subtracting the domain P5: evidence of the relaxation domain P6 (local electron hopping).

Permittivity Nyquist plots of $Li_{2.12}Co_{0.44}N$

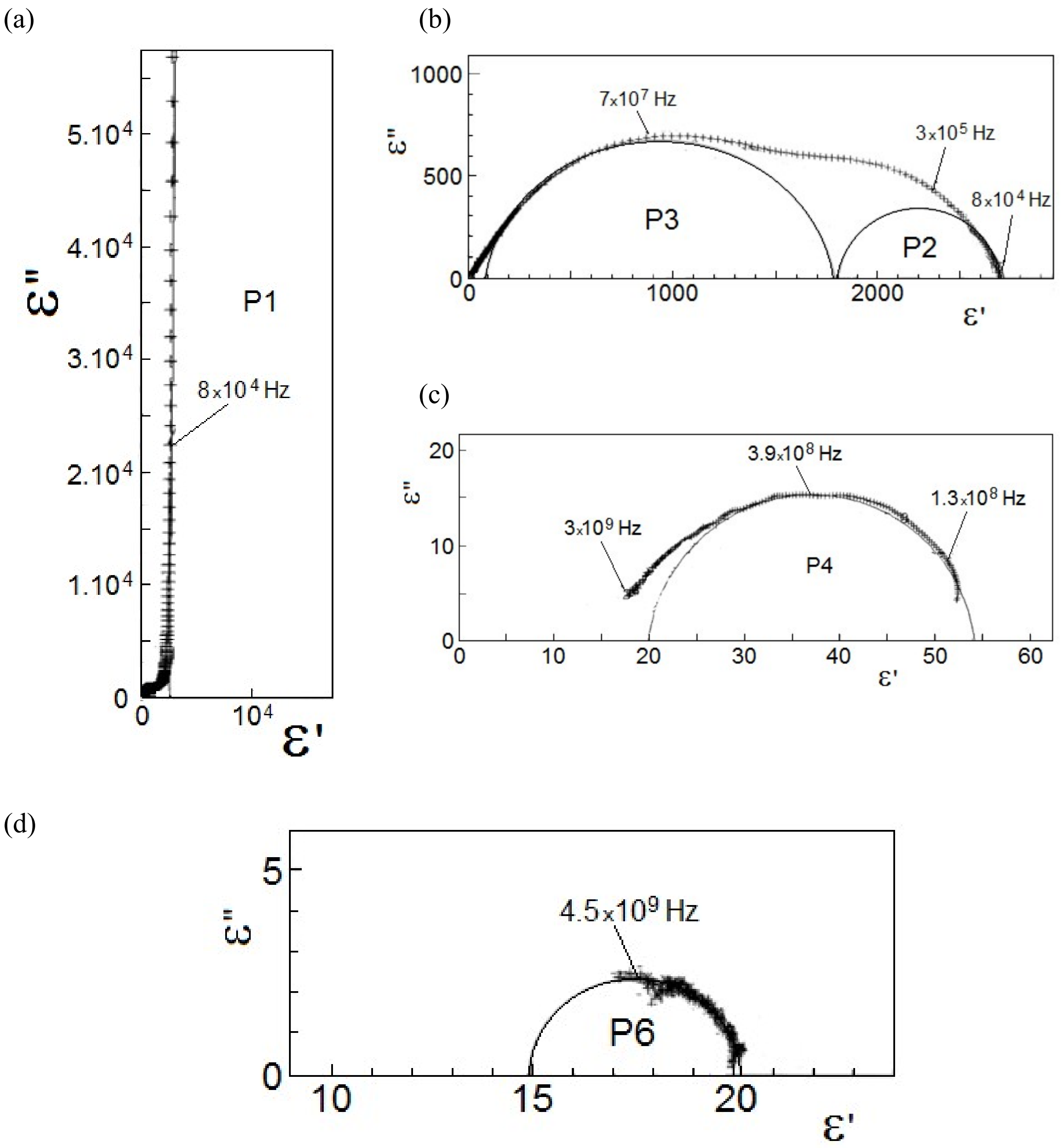

Figure S7. Nyquist plots of the imaginary part ε"(ω) vs. the real part ε'(ω) of the complex permittivity at 300 K for the sample $Li_{2.12}Co_{0.44}N$: a) entire plot from 40 to 10^{10} Hz: only the low frequency contribution P1 is visible; b) plot obtained upon subtracting the domain P1: evidence of the relaxation domains P2 (sample polarization) and P3 (particle polarization); c) plot obtained upon subtracting domains P2 and P3: evidence of the relaxation domain P4 (grain polarization); d) plot obtained upon subtracting the domain P4: evidence of the relaxation domain P6 (local electron hopping).

Summary of the interfacial contributions

Table S1. Space-charge dielectric relaxations contributions (sample, particle and grain polarizations) at room temperature. s is the parameter of the power-law term $A(i\omega)^{s-1}$ of the lower frequency part of the complex permittivity (see expression 7 in the manuscript). ν_s, ν_p and ν_g are the relaxation frequencies of sample, particle and grain polarizations, respectively. ν_{0g} and E_g are respectively the prefactor and the activation energy of ν_g. $\Delta\varepsilon_s$, $\Delta\varepsilon_p$ and $\Delta\varepsilon_g$ are the dielectric strengths of sample, particle and grain polarizations, respectively.

$Li_{3-2x}Co_xN$	**Low-frequency** Power law P1	**Sample** P2	**Particle** P3	**Grain** P4	
	s	ν_s (Hz) $\Delta\varepsilon_s$	ν_p (Hz) $\Delta\varepsilon_p$	ν_g (Hz) $\Delta\varepsilon_g$	ν_{0g} (Hz) E_g (eV)
Li_3N **x = 0.00***	0.30	1.0×10^5 90	4.0×10^6 90	5.0×10^7 14	4.1×10^{12} 0.28
$Li_{2.90}Co_{0.05}$ **x = 0.05***	0.45	1.7×10^3 1700	2.0×10^6 123	2.0×10^7 17	6.0×10^{12} 0.31
$Li_{2.76}Co_{0.12}N$ **x = 0.12***	0.06	4.0×10^3 800	6.3×10^4 3300	1.3×10^7 160	6.1×10^{12} 0.33
$Li_{2.64}Co_{0.18}N$ **x = 0.18***	0.06	1.4×10^4 100	3.0×10^5 1000	7.0×10^7 80	4.7×10^{12} 0.28
$Li_{2.50}Co_{0.25}N$ **x = 0.25***	0.01	2.0×10^3 2000	3.4×10^5 3000	1.8×10^8 83	1.1×10^{13} 0.29
$Li_{2.36}Co_{0.32}N$ **x = 0.32****	0.02	3.0×10^4 1100	4.0×10^5 3900	5.0×10^7 80	1.3×10^{12} 0.26
$Li_{2.22}Co_{0.39}N$ **x = 0.39****	0.01	8.0×10^4 400	1.0×10^6 4780	1.0×10^8 94	9.0×10^{11} 0.23
$Li_{2.12}Co_{0.44}N$ **x = 0.44****	0.00	3.0×10^5 800	7.0×10^7 1700	3.9×10^8 34	1.2×10^{12} 0.21

* Ionic conductors; ** Electronic conductors.

S4. Dielectric relaxation and percolation [1]

Inhomogeneous conducting materials have a percolation thresholds which depend largely on their geometries (dimensionality, structure). These materials contain a conductive region mixed with an insulating (or low conductive) region. The conductive region is constituted by clusters in which the charge carriers move freely. The isolated clusters electrically polarized with a dielectric response given by a relaxation whose main parameters are the dielectric strength $\Delta\varepsilon$ (related to the polarization intensity and the cluster size) and the relaxation time τ which corresponds to the transit time from one edge to the other of the cluster.

The dielectric strength $\Delta\varepsilon$ and the relaxation frequency $\nu = 1/2\pi\tau$ of a percolating system are given by the following power law forms [1]:

$$\Delta\varepsilon \sim |\phi - \phi_c|^{-s} \tag{S4.1}$$

$$\nu \sim |\phi - \phi_c|^{s+t} \tag{S4.2}$$

below and above ϕ_c. f is the volume fraction of the conductor, ϕ_c the percolation threshold. s and t are critical exponents.

Below the threshold, the material is an insulator because the clusters are not connected. Thus the size ξ of the clusters increases until some of them become percolated through the sample (at the threshold). The dielectric strength $\Delta\varepsilon$ and the relaxation time τ (i.e. the transit time from one edge to the other of the cluster), which vary in the same way as ξ, tend toward ∞ (or a great value) at the threshold according to the percolation theory (see Fig. 9d and 9e of the manuscript). The relaxation frequency $\nu = 1/2\pi\tau$ tends thus toward zero (or a minimum value) at the threshold.

[1] A.L. Efros, B.I. Shklovskii. *Phys. stat. sol. (b)*, 1976, **76**, 475-485

Above the threshold, the material is conductor with connected clusters throughout its volume. However, as some isolated clusters remain in the material their size ξ, dielectric strength $\Delta\varepsilon$ and τ decrease sharply according to the percolation theory. Thus, the relaxation frequency ν increases sharply (see Fig. 9d and 9e of the manuscript). These behaviors correspond to a sharp diminution of the size and the number of isolated clusters.